JOURNAL OF MATERIALS SCIENCE **35** (2000) 3983–3988

Effects of processing history on thermal debinding

A. BANDYOPADHYAY
School of Mechanical and Materials Engineering, Washington State University, Pullman, WA 99164-2920, USA
E-mail: amitband@mme.wsu.edu

S. C. DANFORTH, A. SAFARI
Department of Ceramic and Materials Engineering, Rutgers, The State University of New Jersey, Piscataway, NJ 08854, USA

Thermal debinding behavior of silicon nitride parts processed via fused deposition of ceramics (FDC) and extrusion was studied. Heating rate, holding time, setter bed chemistry were some of the variables that were studied to understand their effect on green ceramic parts. Effect of processing history on the binder loss, porosity development and binder distribution profiles were examined on partially binder-burned-out samples. Results show that prior processing history has significant impact on binder distribution profiles and binder loss behavior.

1. Introduction

Ceramic powders require processing aids such as binders, dispersants, and plasticizers during forming to maintain the shape of the desired components. Though the organic additives help forming process, they must be removed completely prior to densification to prevent degradation of final properties [1]. Among the various binder removal techniques for ceramic components, thermal debinding remains the most widely used process and, in most cases, the slowest step in the ceramic manufacturing process. Significant effort has been performed on thermal debinding process for metal and ceramic parts to understand various mechanisms [2–11]. In this work, the effect of processing history on the thermal debinding of silicon nitride components was studied. Parts processed via FDC were compared to single screw extruded parts. Heating rate, setter bed chemistry, soaking or holding time were varied to understand their effects during thermal debinding.

1.1. Fused deposition of ceramics

Fused deposition of ceramics (FDC) is one of the solid freeform fabrication (SFF) techniques that is based upon commercial FDM™ technology (Stratasys™ Inc., Eden Prairie, MN). Over the last decade, SFF techniques have been developed to produce polymer, metal or ceramic components directly from a computer aided design (CAD) file without using any part-specific tooling, dies or molds [12–17]. The FDC process was developed to produce functional-quality ceramic components from a CAD data file. Fig. 1 shows a schematic of the FDC process. Spooled green ceramic filaments (50 to 60 vol% ceramic powder; remainder thermoplastic binder) of 1.75 mm nominal diameter are fed into a heated liquifier via a set of computer-driven rollers. The liquifier, whose motion is computer controlled in the X-Y plane, extrudes materials through a nozzle and deposits them on a fixtureless platform. The fixtureless platform moves in the Z direction. Commercially available FDM™ machines build polymer parts with polymer filaments, as opposed to ceramic powder-loaded filaments for FDC. The liquefier temperature is set slightly above the melting point of the green ceramic filaments. The filament softens and melts inside the liquefier. The cold filament at the top of the liquefier acts as a piston, as in a direct piston extrusion process, and creates a positive pressure to extrude the molten material out of the liquefier through the nozzle. The nozzle diameter varies from 0.25 to 1.3 mm in the commercially available machines. Computer-driven counter-rotating rollers control the filament feed rate. After the deposition of one layer is complete, the fixtureless platform indexes down by one layer (between 0.2 to 0.5 mm) and the next layer is built on the previous layer. The part building process continues until the component fabrication is complete. Like ceramic injection molded parts, green ceramic parts processed via FDC contain approximately 40 to 50 vol% thermoplastic binders. Crack free debinding is an integral part of the post processing steps. The thermal debinding process has been used for binder removal of FDC parts.

Understanding the influence of layered manufacturing on thermal debinding was the main objective of this work. In this work FDC parts processed via layer-by-layer manufacturing process, were compared with extruded parts processed via conventional manufacturing processes. The ceramic powder and binder compositions of all samples were the same for both FDC and extruded parts.

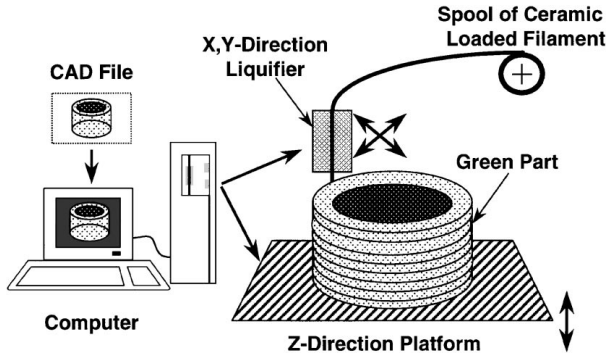

Figure 1 Schematic of FDC process.

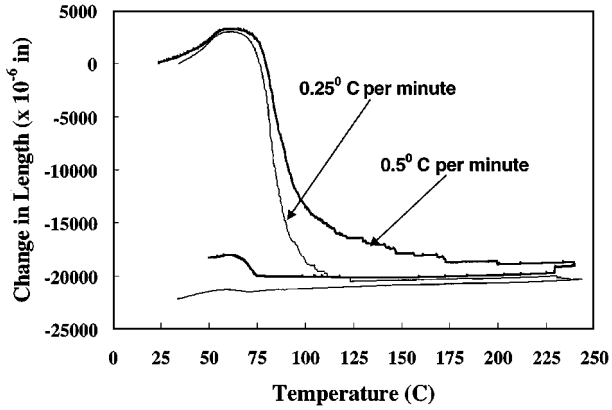

Figure 2 Dilatometry studies of extruded ceramic bars at different heating rates in furnace air environment.

2. Experimental procedure

Green ceramic parts were processed via FDC and single-screw extrusion processes. As-received GS 44 silicon nitride powders (AlliedSignal Ceramic Components, Torrence, CA) were ball milled and coated with a surfactant, 3 weight % oleyl alcohol (Fisher Scientific) in ethyl alcohol (Fisher Scientific), to reduce the agglomeration and improve the ceramic powder distribution in the binder. A four-component commercial thermoplastic binder, ICW (Stratasys® Inc., Eden Prairie, MN), was used for this study. The ICW material was developed by Stratasys® and made commercially available to build polymer parts using FDM machines. The ICW polymer was used as a binder for both FDC and extruded parts as the chemistry was already tailored for fused deposition based technology. The GS 44 silicon nitride powders were compounded with ICW binder at 100°C using a HAAKE system 9000 Rheocord torque rheometer (Haake Fision Instruments, Paramus, NJ). The compounded and granulated mix was fed into Haake single screw extruder attached to a HAAKE system 9000 Rheocord torque rheometer. For FDC, continuous lengths of 1.75 cm $\pm$ 0.003 cm diameter flexible filaments were horizontally extruded with the single screw extruder through a capillary die of 1.75 cm diameter. For extruded samples, continuous lengths of 1.25 cm $\times$ 1.25 cm bars were extruded using a single screw extrusion process. Green ceramic parts were processed via FDC using a 3D Modeler™ FDM machine. The build-temperature was varied between 150 to 190°C; the nozzle diameter was 400 μm. A slice thickness of 250 μm was used for all parts. Thermal debinding was carried out under flowing nitrogen environment (12 cm^3/minute) for all samples to avoid surface oxidation of the silicon nitride powder. The influence of different variables, such as heating rate, soaking time, sample size, setter bed chemistry and processing history of the samples were studied. A two-stage cycle was used; in stage I the majority of the binder was removed under flowing nitrogen and in stage II residual carbon was removed under an oxidizing air environment. Sintering of GS-44 Si_3N_4 parts was performed at AlliedSignal (Morristown, NJ) using a gas pressure sintering cycle that utilized an overpressure of nitrogen to prevent decomposition. After sintering the density, shrinkage and four point bend flexural strengths of FDC and extruded samples were measured. These data are reported elsewhere [15].

3. Results and discussion

3.1. Binder burn out cycle development

Development of the binder burn out cycle for green ceramic parts started with thermogravimetric analysis (TGA) of pure ICW binder. The TGA plot of ICW binder shows that weight loss starts around 100°C and continues to 550°C at a heating rate of 10°C per minute in a nitrogen environment. Dilatometry studies were performed on extruded green ceramic bars with 60 volume fraction solids loading. The bars were 25 mm long and of 6 $\times$ 6 mm^2 cross-sectional area. Samples were heated to 250°C at different heating rates and cooled to room temperature in a single push-rod Theta dilatometer. Change in length as a function of sample temperature was measured. It can be seen from Fig. 2 that initially there was an expansion followed by a contraction in sample length. The expansion starts at 65°C, which matches the softening temperature of ICW binder. Sample expansion continues to 75°C, where a contraction begins. The contraction in liquid binder containing ceramic samples occurs by particle rearrangements under small pressure from the push rod of the dilatometer. Pure ICW binder melts at 68–70°C, which promotes the particle migration at 75°C. The rate at which particle rearrangements take place is a time-dependent process, which is evident in Fig. 2. For the sample heated at a rate of 0.25 degrees C/minute, particle rearrangement was over by 125°C, whereas for a similar sample heated at a faster rate (0.5 degrees C/minute), particle rearrangement continued to 175°C. Once the particle rearrangement was over, change in length was negligible. Particle rearrangement is an irreversible process. When rearrangements occurs, excess binder wicks from the center of the sample to the exterior. After this stage, the surface color of all samples changes and the binder-rich surfaces can be observed. During cooling, there is an uniform contraction of the samples.

A three-stage heating cycle was developed for FDC and extruded parts; stage 1 was from room temperature to 150°C, stage 2 from 150°C to 350°C and stage 3 from 350°C to 450°C. Heating rates and holding times for each stage were optimized for defect-free thermal debinding of FDC and extruded parts. Among the three stages, stage 1 was the binder softening zone, during which large external cracks formed; during stage 2 the majority of the binder left the system via

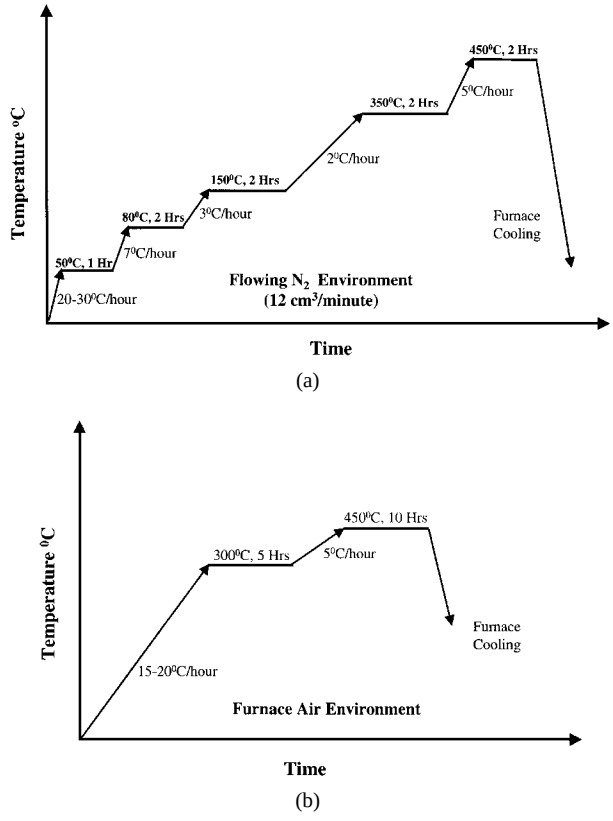

Figure 3 Schematic of a working binder burn out cycle (a) First cycle in N_2 environment and (b) Second cycle in furnace air environment.

capillary-driven liquid binder migration and diffusion-controlled evaporation. Internal cracks formed during this time. Once the part reached stage 3, it had developed an internal-networked pore structure, and binder removal was comparatively easier.

After trying various heating rates, a working binder-removal cycle was developed with heating rates of 3 °C/hour from 80°C to 150°C, 2 °C/hour from 150°C to 350°C and 5 °C/hour from 350°C to 450°C. The environment was flowing nitrogen and sample size could be as large as 12 mm × 12 mm cross-section. Over 75% of the binder was removed during this cycle. In a second heating cycle, samples were heated in a furnace air environment at a heating rate of 5 to 10 degrees C/hour from room temperature to 500°C for complete removal of binders and residual carbons. Soaking times were based on the part sizes, and varied between 5 to 10 hours. Fig. 3a and b show the schematic of the thermal debinding cycles for FDC and extruded parts.

Experiments were conducted to understand the effects of various types of setter materials. Porous zirconia plate (Selee Corporation, NC), alumina powders and activated carbon (40 to 300 mesh, Fisher Scientific) showed the best results. Alumina and activated carbon powders showed better performance over porous zirconia plate, but some of the alumina powders adhered to the silicon nitride surfaces after binder removal. Those residual powders were difficult to remove. Alumina powders reacted during sintering of silicon nitride parts and caused contamination. Activated carbon was used as a setter powder for all the test samples. Samples were completely embedded in activated carbon powders and heated in flowing nitrogen environment.

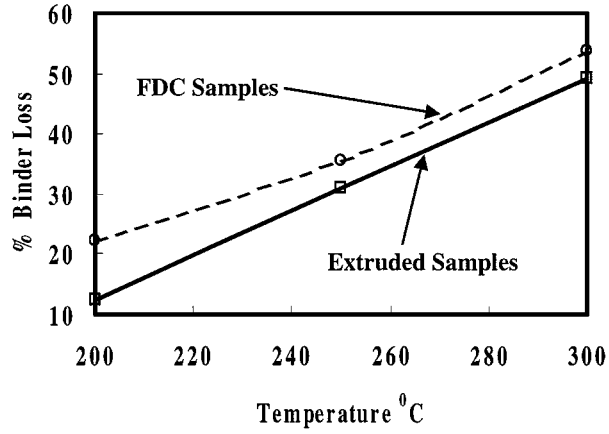

Figure 4 Effect of prior processing history on binder loss.

3.2. Effects of processing history on binder removal

The aim of this study was to compare the effects of processing history on thermal debinding of silicon nitride parts. The effects were monitored through change in binder loss, porosity development and binder distribution profiles of partially and fully debinded samples.

3.2.1. Binder loss

Fig. 4 shows the effects of processing history on the binder loss at different temperatures. When extruded and FDC samples of same sizes were compared, it was observed that the binder loss for FDC samples was always more than that of the extruded bars at a fixed temperature. Moreover, the difference was more prominent at low temperatures when the binder loss mechanism was primarily controlled by liquid binder migration via capillary action or wicking. At higher temperatures, at which the binder removal mechanism changes to diffusion-controlled binder evaporation, the difference in binder loss decreases. But in all the cases, FDC samples showed greater total binder loss compared to the extruded samples. The reason for greater binder loss with FDC samples could be due to the presence of micro-porosity and/or a porosity gradient due to layered manufacturing. Increasing the amount of binder loss for FDC parts over extruded parts is beneficial because it reduces the chances of cracking for the FDC parts.

3.2.2. Porosity development

Porosity development is one of the most significant events during binder burn out. Once a continuous network of porosity develops inside the sample, binder-removal occurs without causing cracking to the part. A faster heating rate can be applied during this stage for thermal debinding. Development of open porosity starts with the diffusion-controlled binder removal process. The open porosity front starts moving from the surface to the inside of the part and the evaporated binder diffuses from inside to the surface. For multicomponent binder systems, higher-melting binder components form a skin near the surface and act as a barrier for the diffusion of evaporated species.

Various research groups have proposed different models for the mechanisms of binder front development. German [2] have developed models in which pore

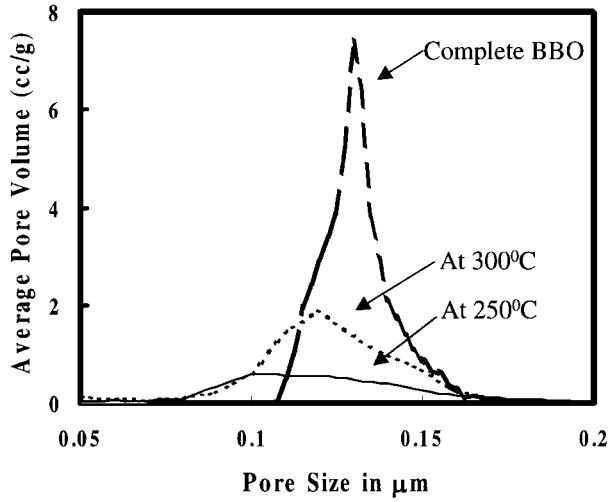

Figure 5 Pore evolution of FDC parts during binder burn out.

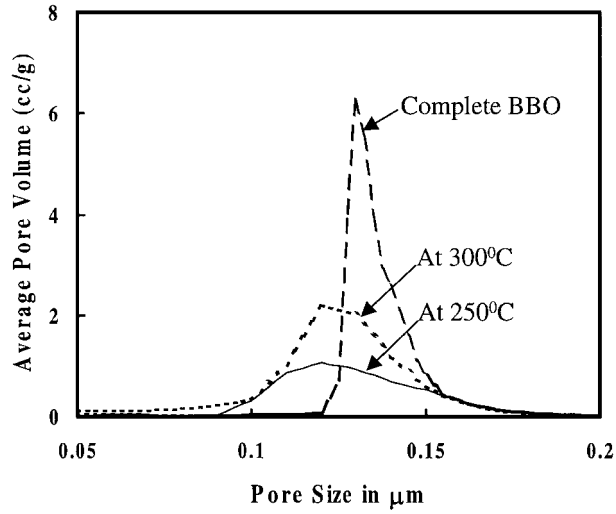

Figure 6 Pore evolution of single-screw extruded parts during binder burn out.

development was modeled as a receding planar front, ignoring the capillary redistribution of binders. Transport of volatile species through binder-filled pores was also ignored in these models. Matar *et al.* [18] developed a model on the porosity development that quantifies the degradation and diffusion of organic vehicle during thermal debinding of injection molded metals or ceramics. Lewis and Cima [19] showed that transport of volatile species in binder-filled pores occurs by diffusion and is the rate limiting factor during debinding of closed pore compacts. It has been reported that small pores tend to draw liquid binder via capillary action from the larger pores until they become filled [20]. As a result, larger pores debind prior to the smaller pores.

Porosity measurements were conducted on samples after partial and complete binder removal using mercury intrusion porosimetry (Micromeretics Auto-Pore III) to reveal the effect of processing history on pore development. Fig. 5 shows the mercury intrusion porosimetry plot for FDC samples after partial and complete binder removal at different temperatures. Samples were heated to that temperature and held for one hour, then furnace-cooled. Three observations that can be deduced from Fig. 5 are (i) no significant porosity development occurred in the samples below 200°C; (ii) average pore size remained constant during porosity development and (iii) as temperature increased, average pore volume increased. The average pore size in the samples remained in the range of 0.1 to 0.15 μm. Fig. 6 shows a porosity distribution plot for the single screw-extruded samples. The average pore size for the extruded bars ranged from 0.05 to 0.2 μm. For both cases, porosity development did not start below 200°C. These results indicate that the development of porosity is more dependent on particle size, binder chemistry, solids loading and furnace environment than processing history of green parts.

3.2.3. Binder distribution

Most of the investigations on binder distribution during binder removal characterized binder migration as capillary or diffusion-controlled evaporation processes that occurred during the binder burn out cycle. In this work, binder distribution profiles in samples from which binder had been partially removed were characterized using optical and stereo microscopes. Polished cross sections of partially-debinded samples showed a contrast between binder-rich regions and the powder-rich regions. Fig. 7a and b show the binder distribution in single-screw and FDC bars, heated to 250°C and

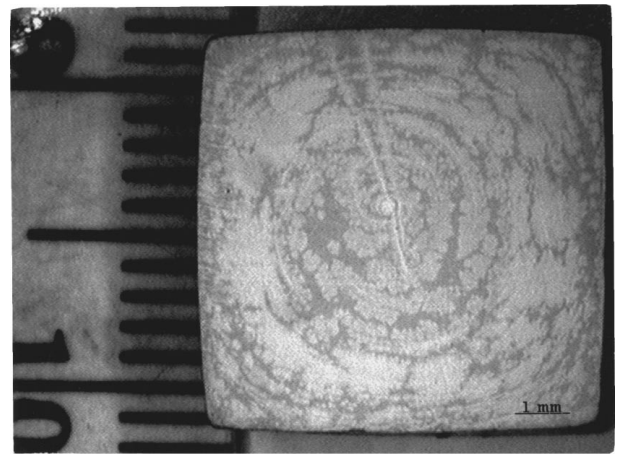

(a)

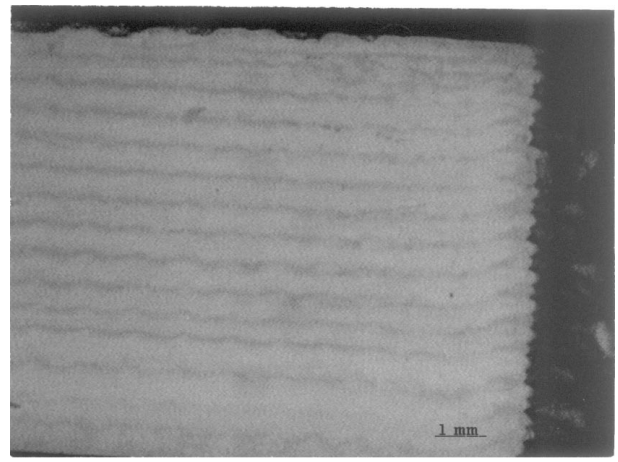

(b)

Figure 7 Optical photomicrographs of binder distribution profiles of partially binder burned out samples at 250°C. (a) Single screw extruded bar; (b) FDC bar.

held for 1 hour. The dark regions are binder-rich and the brighter regions are powder-rich areas. The TGA results showed that the darker regions had at least 4 weight % higher binder concentration than the brighter regions. This was sufficient to cause the contrast in appearance of the cross sections of different samples. It has been reported that the movement of liquid binder occurs due to local variation of particle packing that causes a variation in the pore suction pressure [19]. Smaller pores produce a larger suction pressure than bigger pores and cause a liquid migration from the bigger pores to the smaller pores [20–23]. The phenomenon is treated by the Young and Laplace equation:

$$P_s = \frac{2\gamma}{r}$$

where r is the pore radius, γ is the liquid vapor interfacial energy and P_s is the suction pressure. The difference in the structure of the binder distribution pattern shown in Fig. 7a and b was primarily due to the effects of the processing history. Fig. 7a shows a spiral pattern of binder-rich regions caused by the bars being extruded via single screw extrusion process. During single screw extrusion, compounded materials were mixed using a rotating screw that pushed the material forward towards the die. Fig. 7b shows the binder distribution

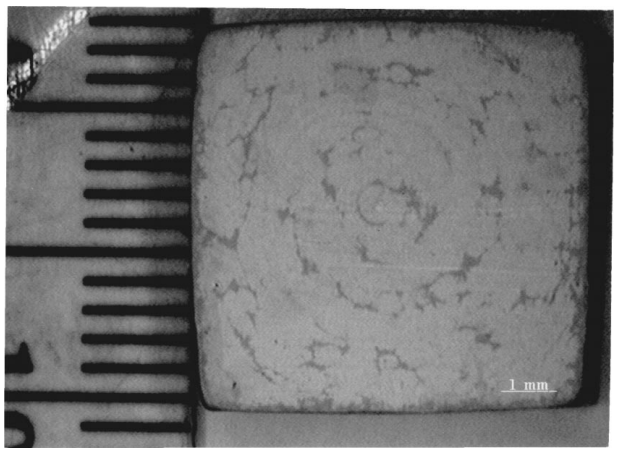

(a)

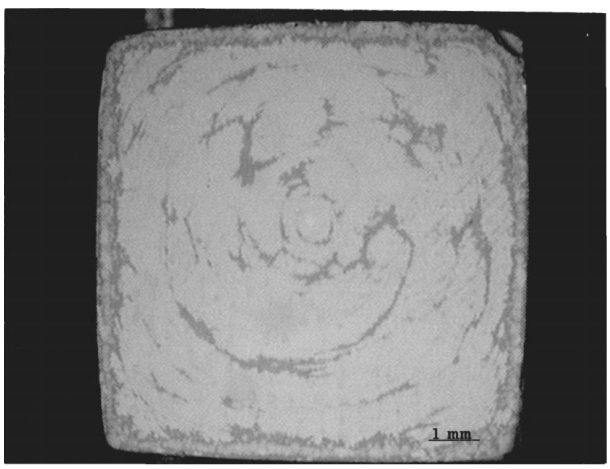

(b)

Figure 8 Optical photomicrographs of binder distribution profiles of single screw extruded bars showing the effect of hold time; (a) 1 hour at 250°C and (b) 10 hours at 250°C.

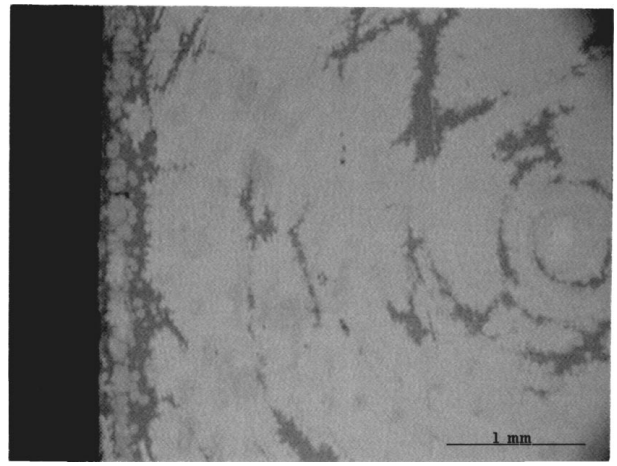

Figure 9 Optical photomicrograph of binder distribution profiles of partially binder burn out single screw extruded bar at 300°C for one hour.

for the FDC samples. These samples were produced via layer-by-layer deposition. A preferential layer-wise segregation of the binder rich regions was an artifact of prior processing history. Moreover, the waviness in the binder-rich layers is a signature of individual roads that were built next to each other. Information about the road width and layer thickness during fabrication of FDC parts can be measured from this binder distribution.

Fig. 8a and b show the effects of the holding time on the binder distribution of single screw extruded bars. Fig. 8a shows the binder distribution profile of a sample that was held at 250°C for 1 hour and Fig. 8b for a sample at 250°C for 10 hours. With increasing time, the binder diffused from the inside to the outside. The increased holding time increased the separation between the binder-rich regions in the part. Moreover, as more binder was leaving the part, the amount of binder-rich regions also decreased. The effect of temperature is shown in Fig. 9, for which the sample was held at 300°C for 10 hours. Though some pockets of binder-rich regions can be seen inside the sample with a binder-rich skin, the amount of binder-rich area was reduced significantly by binder loss at a higher temperature. If an internal crack forms during thermal debinding, a binder-rich region develops around the crack because of the open surfaces. The binder distribution profiles of these samples were visible only after the samples were held above 200°C. Below 200°C, no contrast between binder-rich and powder-rich areas could be identified. These data indicate that development of binder distribution profiles is linked to the pore evolution of thermal debinding.

4. Conclusions

Effects of processing variables on thermal debinding of green silicon nitride ceramic parts were studied. Green ceramic parts were processed by FDC, one of the layered manufacturing techniques and by single screw extrusion processes. Thermal debinding cycles for 1.25 cm × 1.25 cm cross-section parts were developed with heating rates as low as 2°C/hour. Setter powder, heating rate and holding times were found to have significant impact on the binder removal process. It was

observed that prior processing history had significant effects on the binder distribution profiles during thermal debinding. A spiral binder distribution profile was seen for the partially debinded single-screw-extruded samples in contrast to the layered structure of FDC parts of the same compositions.

Acknowledgements

The authors would like to acknowledge the financial support from DARPA/ONR/AlliedSignal (contract No. N00014-94-0115) and ONR-YIP grant (N00014-98-1-0550). The authors would like to thank Drs. M. K. Agarwala, P. Bhargava, S. Rangarajan, P. J. Whalen and Mr. P. Teung of Rutgers University and Mr. K. Kerstetter of WSU for their technical and experimental assistance during various stages of this research.

References

1. J. A. LEWIS, *Annual Rev. Mater. Sci.* **27** (1997) 147.
2. R. M. GERMAN, *Int. J. Power Metall.* **23** (1987) 237.
3. M. J. CIMA, J. A. LEWIS and A. D. DEVOE, *J. Amer. Ceram. Soc.* **72** (1989) 1192.
4. M. R. BARONE and J. C. ULICNY, *ibid.* 73 (1990) 3323.
5. Y. BAO and J. R. G. EVANS, *J. Europ. Ceram. Soc.* **8** (1991) 81.
6. R. M. GERMAN, "Powder Injection Molding" (Metal Powder Industries Federation, Princeton, NJ, 1990) p. 95.
7. K. E. HRDINA and J. W. HALLORAN, *J. Mater. Sci.* **33** (1998) 2805.
8. M. J. EDIRISINGHE, *Proc. Br. Ceram. Soc.* **54** (1990) 109.
9. G. BANDYOPADHYAY and K. W. FRENCH, *J. Europ. Ceram. Soc.* **11** (1993) 23.
10. P. CALVERT and M. CIMA, *J. Amer. Ceram. Soc.* **73** (1990) 575.
11. J. WOODTHROPE, M. J. EDIRISINGHE and J. R. G. EVANS, *J. Mater. Sci.* **24** (1989) 1038.
12. M. L. GRIFFITH and J. W. HALLORAN, *J. Amer Ceram. Soc.* **79**(10) (1996) 2601.
13. P. K. SUBRAMANIAN, G. ZONG and H. L. MARCUS, in Proceedings of the Solid Freeform Fabrication Symposium, The University of Texas at Austin, August 3–5, 1992, edited by H. L. Marcus, J. J. Beaman, J. W. Barlow, D. L. Bourell and R. H. Crawford, Vol. 1992, p. 63.
14. C. GRIFFIN, J. DAUFENBACH and S. MCMILLIN, *Amer. Ceram. Bulletin* **73** (1994) 109.
15. M. K. AGARWALA, A. BANDYOPADHYAY, R. VAN WEEREN, P. WHALEN, A. SAFARI and S. C. DANFORTH, *ibid.* **11** (1996) 60.
16. J. W. COMB and W. R. PRIEDEMAN, in Proceedings of the Solid Freeform Fabrication Symposium, The University of Texas at Austin, August 3–5, 1992, edited by H. L. Marcus, J. J. Beaman, J. W. Barlow, D. L. Bourell and R. H. Crawford, Vol. 1992, pp. 86–91.
17. A. BANDYOPADHYAY, R. K. PANDA, V. F. JANAS, M. K. AGARWALA, S. C. DANFORTH and A. SAFARI, *J. Amer. Ceram. Soc* **80** (1997) 1366.
18. S. A. MATAR, M. J. EDIRISINGHE, J. R. G. EVANS and E. H. TWIZELL, *J. Mater. Res.* **8** (1993) 617.
19. J. A. LEWIS and M. J. CIMA, *J. Amer. Ceram. Soc.* **73** (1990) 2702.
20. G. W. SCHERER, *ibid.* **73** (1990) 3.
21. N. H. CEAGLSKE and O. A. HOUGEN, *Trans. Amer. Inst. Chem. Engg.* **33** (1937) 283.
22. T. M. SHAW, *Physical Review Letters* **59** (1987) 1671.
23. *Idem., J. Amer. Ceram. Soc.* **69** (1986) 27.

Received 22 September 1999
and accepted 7 February 2000